Macromolecules

COMMUNICATION TO THE EDITOR

pubs.acs.org/Macromolecules

Indacenodithiophene-*co*-benzothiadiazole Copolymers for High Performance Solar Cells or Transistors via Alkyl Chain Optimization

Hugo Bronstein,[†] Dong Seok Leem,[†] Richard Hamilton,[‡] Paul Woebkenberg,[†] Simon King,[†] Weimin Zhang,[†] Raja Shahid Ashraf,[†] Martin Heeney,[†] Thomas D. Anthopoulos,[†] John de Mello,[†] and Iain McCulloch*[,†]

[†]Department of Chemistry, Centre for Plastic Electronics, Imperial College London, London SW7 2AZ, U.K.

[‡]Solar Press, 2 Royal College Sreet, London NW1 0NH, U.K.

Supporting Information

Initially, the role of an alkyl chain on a conjugated polymer was to confer solubility of the rigid-rod-like structure in common organic solvents. It is now apparent that the choice of solubilizing chain can vastly affect the properties of the polymer, as it can be used to tune a materials' crystallinity in the solid state as well as its miscibility with other materials in thin film blends. The latter of these is of extreme importance in the field of OPV where the extent of phase separation between a donor conjugated polymer and a fullerene acceptor is a critical factor in determining solar cell performance.[1−5]

Yang et al. studied the effects of side chain variation on a naphtho[2,1-*b*:3,4-*b*′]dithiophene-*co*-4,7-di(thiophen-2-yl)benzothiadiazole system[6] and observed differences in the V_{oc} and J_{sc}. These were quantitatively correlated with a pre-exponential dark current term, which they claimed accounts for the intermolecular interactions in the polymer/fullerene blend. Biniek et al. studied the effect of side chain variation and site of attachment on a benzo[1,2-*b*:4,5-*b*′]dithiophene-*co*-thieno[3,4-*b*]thiophene polymer.[7] They found an increased solar cell efficiency using ethylhexyl chains over linear dodecyl chains. Szarko et al. very recently reported on the effect of side chain variation on thieno[3,-*b*]thiophene-*co*-benzodithiophene polymer systems, which have given record breaking (∼8%) PCEs.[8] They found that varying the degree of alkyl chain branching affected the $\pi-\pi$ stacking distance which they suggested allowed a varying amount of fullerene intercalation to occur. A study on the variation of the side chain on the acceptor portion of a *N*-alkylthieno[3,4-*c*]pyrrole-4,6-dione polymer demonstrated that the highest solar cell efficiency was achieved with a linear chain.[9]

Recently, we reported the synthesis and high hole mobility of an indacenodithiophene-*co*-benzothiadiazole (IDT−BT) copolymer with hexadecyl alkyl chains **P4**.[10] The long linear alkyl chains were attributed to impart some degree of crystallinity in thin film. Chen et al. demonstrated the high performance of a similar IDT−BT copolymer bearing phenylhexyl side chains in solar cell devices.[11] Replacement of benzothiadiazole on this system with alternative acceptors has also yielded efficient solar cells.[12] We were interested in investigating the role the solubilizing chains play in the performance of this low-band-gap polymer in both TFT and OPV devices. The effect of varying the alkyl chain from short and branched (methylbutyl) to long and linear (hexadecyl) on the optical and electronic properties is presented here.

Copolymers **P1**−**P4** were synthesized via Suzuki couplings using previously reported conditions.[10] It was not possible to achieve high molecular weights with the methylbutyl side chains **P1** due to precipitation of the polymer during polymerization, a consequence of its lower solubility. The remaining polymers were synthesized in high molecular weights, as expected, due to the enhanced solubilizing effect of the longer alkyl chains (Table 1).

The solution and thin film UV−vis absorption spectra are shown in Figure 1. In solution, polymers **P2**−**P4** display very similar absorption maxima at around 660 nm. The absorption maxima of **P1** is at a slightly shorter wavelength (645 nm) which is attributed to the lower molecular weight of the material. In all polymers a slight shoulder can be observed at a shorter wavelength, which is attributed to solution aggregation. In thin film, polymers **P1**, **P3**, and **P4** display red-shifted absorbance maxima (∼10−15 nm). Furthermore, the shoulder at a shorter wavelength (∼575 nm) is clearly more pronounced for all polymers which is attributed to solid state aggregation, which has been demonstrated previously for **P4**. In contrast, there is no significant red-shift in the absorbance of **P2**, and there is only a slight shoulder observed at shorter wavelengths, perhaps due to a lack of thin film crystallinity and subsequent backbone planarization. The HOMO energy levels were measured by PESA (photoelectron spectroscopy in air), and the small variations were believed to be due to the standard error in the measurement rather than an actual difference in the energy levels of the polymers. The LUMO was estimated by addition of the optical band gap (absorption edge of the thin film UV−vis absorption spectra) to the measured HOMO values.

Bottom-contact, top-gate architecture field effect transistors were fabricated from **P1**−**P4**, and the details are collected in Table 2. **P2**−**P4** all display extremely high hole mobility (>0.1 $cm^2 V^{-1} s^{-1}$), the highest of which is the material with the longest alkyl chains (**P4**). The slightly lower mobility of **P3** which also contains linear alkyl chains can be attributed to the difficulty in obtaining good quality films due to the lower solubility of this sample (which arises from its higher molecular weight and the inherent lower solubilizing effect of the shorter linear alky chain). **P1** displayed significantly poorer hole mobility, which is probably, in part, a result of its significantly lower molecular weight. The extremely high hole mobility measured for **P2** is remarkable considering the absence of any observed aggregation effects in the solid-state absorption spectrum and the presence of only short bulky side chains. A similar phenomenon has been observed by Tsao et al., who measured the charge carrier mobilities of a conjugated polymer

Received: May 20, 2011
Revised: August 6, 2011
Published: August 22, 2011

Scheme 1. Synthesis of IDT−BT Copolymers

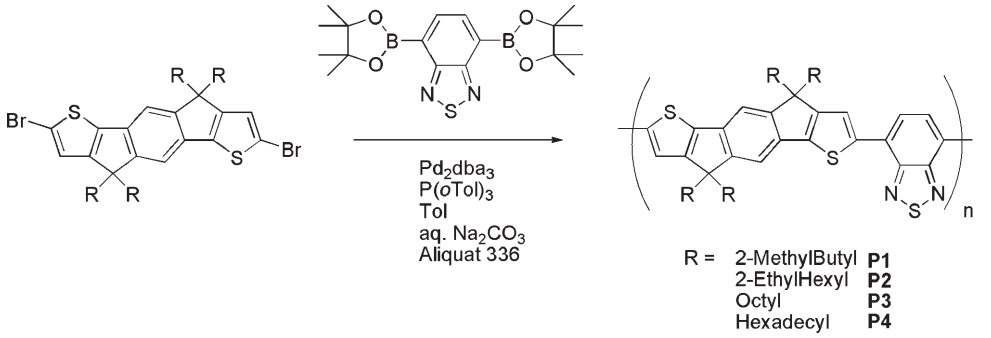

Table 1. Properties of IDT−BT Polymers

polymer	M_n/kDa[a]	M_w/kDa[a]	PDI[a]	λ_{max} (soln)/nm[b]	λ_{max} (film)/nm[c]	HOMO[d]	LUMO[e]
P1	9	13	1.4	645	655	−5.3	−3.6
P2	40	87	2.2	659	660	−5.3	−3.6
P3	33	243	7.4	660	674	−5.3	−3.7
P4	38	108	2.8	663	677	−5.4	−3.7

[a] Estimated by SEC using PS standards and chlorobenzene as eluent. [b] In dilute $CHCl_3$ solution. [c] Spun from chlorobenzene solution (5 mg/mL). [d] Measured by PESA. [e] Addition of absorption onset in thin film UV−vis onto HOMO.

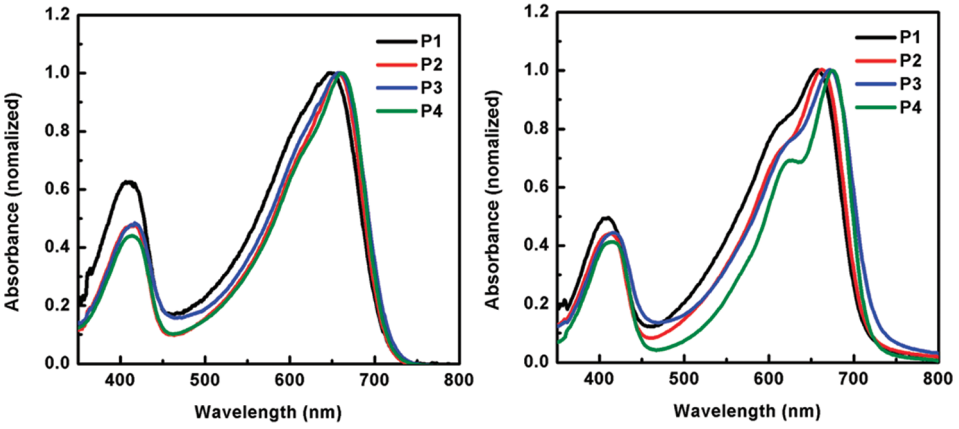

Figure 1. Normalized solution (left) and thin film (right) UV−vis absorption spectra of IDT−BT copolymers. Solution measurements were done in dilute $CHCl_3$. Thin films were spun from a 5 mg/mL solution in chlorobenzene.

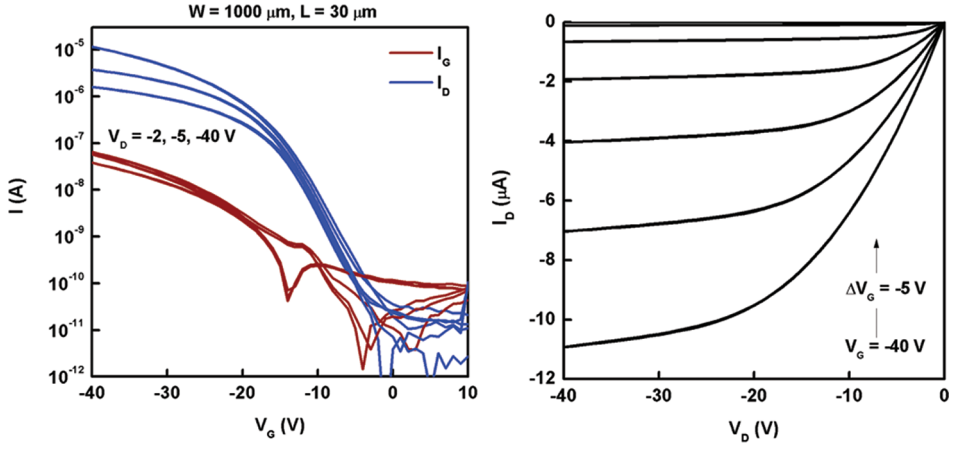

Figure 2. OFET transfer (left) and output (right) curves of **P2**.

dx.doi.org/10.1021/ma201158d |*Macromolecules* 2011, 44, 6649–6652

with either branched or linear alkyl chains and suggested that molecular weight played a more vital role in obtaining high hole mobilities than choice of side chain.[13]

Solar cells with device structure ITO/PEDOT:PSS/polymer (**P1**−**P4**):$PC_{71}BM$/Ca/Al were fabricated, and their averaged properties are shown in Figure 3 and Table 3. The active layers were spin-coated from *o*-dichlorobenzene (ODCB) with a blend of polymer (**P1**−**P4**):$PC_{71}BM$ in a 1:3.5 (w/w) ratio. Devices made from **P1**−**P3** all showed high performance with **P2** giving the highest average PCE of ∼4.5%. The open-circuit voltage (V_{oc}) and fill factor (FF) of all the devices were all comparable, in the range of 0.75−0.79 and 0.44−0.49, respectively. However, it is interesting to note that slightly higher V_{oc} was observed for the branched chain polymers (**P1** and **P2**) than those with linear alkyl chains (**P3** and **P4**). The deep HOMO energy level of this series of polymers allows for the high observed V_{oc}, when used in conjunction with the fullerene acceptor.[14] The short-circuit current (J_{sc}) was significantly more variable with an impressive −11.45 mA cm^{-2} for devices made from **P2**. **P4** had a significantly lower J_{sc} which resulted in the lower observed PCE. A maximum PCE of 5.5% was obtained for **P2** by spin-coating the active layer from a less concentrated solution at a slower spin speed. The increase in PCE is due to an increase in short-circuit current to 13 mA cm^{-2}, and a higher fill factor (0.54), which we believe to be a result of the slower drying of the active layer which allows for formation of a more desirable morphology. Chen et al. observed a significant improvement in fill factor and PCE upon the use of additives or solvent annealing in a similar system with phenylhexyl side chains.[11,15] Further device optimization with the use of additives with these polymers is ongoing.

In order to probe the underlying cause of this significant variation in device performance, AFM images of the devices were recorded (Figure 4). In devices containing **P1**, large crystals of $PC_{71}BM$ can be observed. This causes an extremely high surface roughness to be measured (21.69 nm). In devices containing **P2** and **P3**, a smoother film is observed (surface roughness ∼0.5 nm) where the phase separation appears to be in the nanometer regime.

Table 2. OFET Characteristics of IDT−BT Copolymers

polymer	on/off ratio	max hole μ sat./cm^2 V^{-1} s^{-1}
P1	10^2	0.003
P2	10^5	0.57
P3	10^4	0.15
P4	10^4	1.2

In the case of devices containing **P4**, extremely large (∼300 nm) domains are clearly visible. This unfavorable phase separation is likely to be the cause of the extremely low device efficiency relative to the other materials.

The difference in observed BHJ morphology is attributed to the varying degrees of interaction between the fullerene and the polymer chains. With the short bulky chains (**P1**), there is likely to be insufficient miscibility between the polymer and the fullerene, which results in the formation of PCBM crystallites. It is remarkable that a good PCE is obtained from such an undesirable morphology, although it is possible that enough fullerene is dispersed within the film (it is in significant excess), and the remainder is free to form crystallites. It is clear that a more desirable morphology is obtained with both ethylhexyl and octyl alkyl chains (**P2** and **P3**, respectively). However, it is very interesting to note that despite the similar morphology, a significantly higher PCE is obtained with the ethylhexyl side chains. A possible reason for this could be the increased steric bulk of the ethylhexyl chains which would shield the fused donor portion of the polymer from association with the fullerene. This would result in the fullerene preferentially residing closer to the accepting part of the polymer (i.e., BT) which could facilitate electron transfer onto the fullerene. In the case of the hexadecyl side chain containing polymer (**P4**) the large domains observed can lead to high levels of geminate recombination from isolated donor−acceptor pairs, resulting in low charge separation and device currents. It is interesting to note that there is no correlation between FET mobility and short-circuit current (J_{sc}) as demonstrated by the fact that even the modest hole mobility of **P1** is sufficient to extract charges, resulting in a high efficiency OPV device. In stark contrast, **P4**, which has the highest FET hole mobility, has a significantly reduced short-circuit current, which further demonstrates the vital need for morphological control in polymer:fullerne blend OPV devices.

Table 3. OPV Characteristics of IDT−BT Copolymers[a,b]

polymer	V_{oc}/V	J_{sc}/mA cm^{-2}	FF	PCE (%)
P1	0.78	−9.75	0.49	3.79
P2	0.79	−11.45	0.49	4.46 (5.5)[c]
P3	0.74	−10.05	0.46	3.39
P4	0.75	−2.02	0.44	0.66

[a] Under AM1.5 illumination. ITO/PEDOT:PSS/active layer/Ca/Al device structure. Active layer was polymer:$PC_{71}BM$ (1:3.5 w/w) in ODCB; ∼80 nm layer. [b] Average values. [c] Optimized spin-coating conditions.

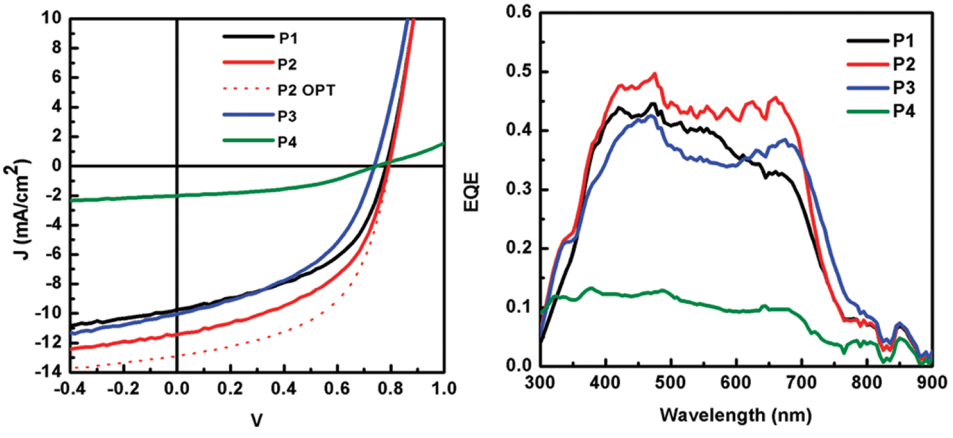

Figure 3. Current density−potential curves for solar cells of IDT−BT copolymers (left) and EQE spectra of devices (right).

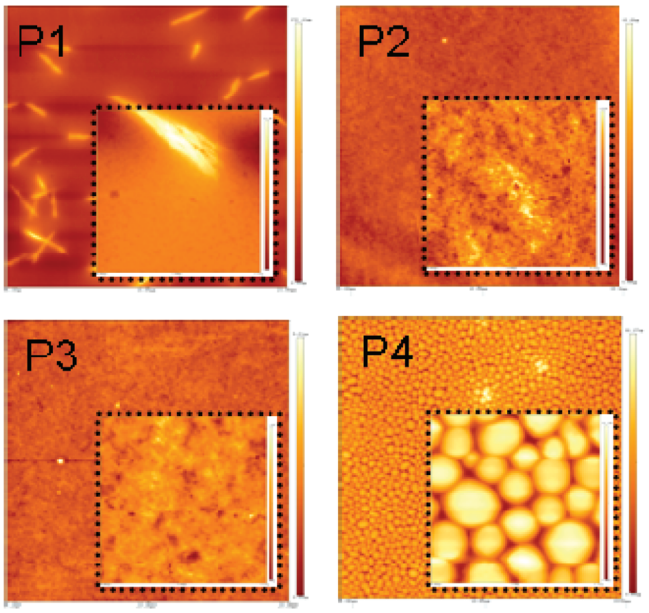

Figure 4. AFM images (tapping mode) of OPV devices. Main 20 × 20 μm, inset 2 × 2 μm.

In conclusion, we have studied how the OFET and OPV performance of a donor−acceptor IDT−BT type polymer is affected by the variation of the solubilizing alkyl chains. For OFETs, a very long linear chain is most beneficial, as this results in the most aggregated solid-state structure (as observed by an increasing amount of a shoulder in the thin film UV−vis spectra). However, extremely high mobilities are also observed in polymers with shorter bulky side chains, which challenges the notion that long linear chains are a necessity in high charge carrier mobility materials. In terms of OPV performance, ethylhexyl side chains lead to very desirable phase separation in this polymer class (as observed by AFM) and extremely good device PCEs. Even shorter and bulkier side chains result in the formation of PCBM crystallites, whereas a long linear chain results in large domains. Further solid-state analysis of the interaction between the polymer side chains and the fullerene acceptor is ongoing and will be presented separately.

■ ASSOCIATED CONTENT

Supporting Information. Synthesis of monomers and polymers; TFT and OPV device fabrication. This material is available free of charge via the Internet at http://pubs.acs.org.

■ AUTHOR INFORMATION

Corresponding Author
*E-mail: i.mcculloch@imperial.ac.uk.

■ ACKNOWLEDGMENT

This work was in part carried out under the EC FP7 ONE-P Project 212311 and DPI Grant 678.

■ REFERENCES

(1) Brabec, C. J.; Heeney, M.; McCulloch, I.; Nelson, J. *Chem. Soc. Rev.* **2011**, *40*, 1185.
(2) Chen, M. H.; Hou, J.; Hong, Z.; Yang, G.; Sista, S.; Chen, L. M.; Yang, Y. *Adv. Mater.* **2009**, *21*, 4238.
(3) Inganas, O.; Svensson, M.; Zhang, F.; Gadisa, A.; Persson, N. K.; Wang, X.; Andersson, M. R. *Appl. Phys. A: Mater.* **2004**, *79*, 31.
(4) Tsao, H. N.; Mullen, K. *Chem. Soc. Rev.* **2010**, *39*, 2372.
(5) Wu, P.-T.; Ren, G.; Jenekhe, S. A. *Macromolecules* **2010**, *43*, 3306.
(6) Yang, L. Q.; Zhou, H. X.; You, W. *J. Phys. Chem. C* **2010**, *114*, 16793.
(7) Biniek, L.; Fall, S.; Chochos, C. L.; Anokhin, D. V.; Ivanov, D. A.; Leclerc, N.; Leveque, P.; Heiser, T. *Macromolecules* **2010**, *43*, 9779.
(8) Szarko, J. M.; Guo, J. C.; Liang, Y. Y.; Lee, B.; Rolczynski, B. S.; Strzalka, J.; Xu, T.; Loser, S.; Marks, T. J.; Yu, L. P.; Chen, L. X. *Adv. Mater.* **2010**, *22*, 5468.
(9) Piliego, C.; Holcombe, T. W.; Douglas, J. D.; Woo, C. H.; Beaujuge, P. M.; Frechet, J. M. J. *J. Am. Chem. Soc.* **2010**, *132*, 7595.
(10) Zhang, W.; Smith, J.; Watkins, S. E.; Gysel, R.; McGehee, M.; Salleo, A.; Kirkpatrick, J.; Ashraf, S.; Anthopoulos, T.; Heeney, M.; McCulloch, I. *J. Am. Chem. Soc.* **2010**, *132*, 11437.
(11) Chen, Y. C.; Yu, C. Y.; Fan, Y. L.; Hung, L. I.; Chen, C. P.; Ting, C. *Chem. Commun.* **2010**, *46*, 6503.
(12) Zhang, Y.; Zou, J.; Yip, H.-L.; Chen, K.-S.; Zeigler, D. F.; Sun, Y.; Jen, A. K. Y. *Chem. Mater.* **2011**, *23*, 2289.
(13) Tsao, H. N.; Cho, D. M.; Park, I.; Hansen, M. R.; Mavrinskiy, A.; Yoon, D. Y.; Graf, R.; Pisula, W.; Spiess, H. W.; Mullen, K. *J. Am. Chem. Soc.* **2011**, *133*, 2605.
(14) Scharber, M. C.; Wuhlbacher, D.; Koppe, M.; Denk, P.; Waldauf, C.; Heeger, A. J.; Brabec, C. L. *Adv. Mater.* **2006**, *18*, 789.
(15) Chan, S. H.; Hsiao, Y. S.; Hung, L. I.; Hwang, G. W.; Chen, H. L.; Ting, C.; Chen, C. P. *Macromolecules* **2010**, *43*, 3399.